ACS APPLIED MATERIALS & INTERFACES

Research Article

www.acsami.org

Electrophoretic Characterization and Purification of Silica-Coated Photon-Upconverting Nanoparticles and Their Bioconjugates

Antonín Hlaváček,[†,‡] Andreas Sedlmeier,[†] Petr Skládal,[‡] and Hans H. Gorris*[,†]

[†]Institute of Analytical Chemistry, Chemo- and Biosensors, University of Regensburg, 93040 Regensburg, Germany

[‡]Central European Institute of Technology (CEITEC), Masaryk University, Brno 625 00, Czech Republic

Supporting Information

ABSTRACT: Photon-upconverting nanoparticles (UCNPs) have attracted much interest as a new class of luminescent label for the background-free detection in bioanalytical applications. UCNPs and other nanoparticles are commonly coated with a silica shell to improve their dispersibility and chemical stability in aqueous buffer and to incorporate functional groups for subsequent bioconjugation steps. The process of silica coating, however, is difficult to control without suitable analytical and preparative methods. Here, we have introduced agarose gel electrophoresis for the analysis and purification of silica-coated UCNPs. The silica shell can be doped with a fluorescent dye for direct detection in the gel without influencing the structure or electrophoretic mobility of the nanoparticles. The preparation of a bare silica shell by reverse microemulsion resulted in individual nanoparticles but also distinct aggregates that could be separated and isolated from the agarose gel. In contrast, the preparation of an ultrathin carboxylated silica shell yielded non-aggregated UCNPs only that could be directly used for protein conjugation. Agarose gel electrophoresis has also facilitated an efficient separation of protein−UCNP conjugates from excess reagents.

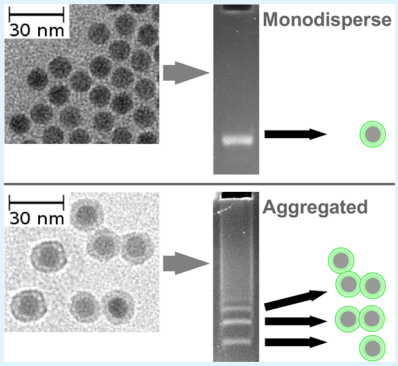

KEYWORDS: *bioconjugation, electrophoresis, nanoparticles, silica coating, upconversion*

1. INTRODUCTION

Photon-upconverting nanoparticles (UCNPs) emit multiple narrow emission bands of higher energy radiation under mild near-infrared (NIR) excitation (anti-Stokes emission), which avoids autofluorescence, light scattering, and absorption of biological materials and enables multiplexed optical encoding.[1−3] The most efficient UCNPs known to date consist of a hexagonal $NaYF_4$ host crystal doped with well-defined amounts of lanthanides, in particular, Yb^{3+} and Er^{3+}. Bright UCNPs that are small (down to 10 nm in diameter) and monodisperse in size are most efficiently prepared in high-boiling organic solvents, such as oleic acid, that result in a hydrophobic surface cover. Bioanalytical applications, however, require a hydrophilic surface to yield stable aqueous dispersions. Generating a well-defined and chemically inert surface structure that confers long-term colloidal stability is still challenging.

Silica coating by water-in-oil (reverse) microemulsions is one of the most frequently used methods for the surface modification of UCNPs and other types of nanoparticles.[4] A stable silica shell renders UCNPs dispersible in water and facilitates the integration of functional groups for subsequent bioconjugation steps. It is important to keep the silica shell as thin as possible to obtain a small luminescent label but also to facilitate applications that are based on luminescence resonance energy transfer.[5] The conditions for the preparation of a homogeneous silica shell that results in monodisperse colloidal nanoparticles in water have to be finely tuned and are not easily controlled.[6] The preparation of a functionalized silica shell is even more challenging.[7−10] Slight variations in the experimental conditions can lead to the enclosure of more than a single nanoparticle in a common silica shell, formation of empty silica nanoparticles, or well-developed but tightly aggregated nanoparticles. Consequently, it is crucial to characterize the result of the silanization process.

Transmission electron microscopy (TEM) and dynamic light scattering (DLS) are the most common methods for the characterization of nanoparticles. TEM, however, is performed on dry nanoparticles *in vacuo* and typically yields no information on the nanoparticle dispersion. Moreover, nanoparticles that form clusters during the drying process are indistinguishable from nanoparticle aggregates that have already formed earlier in dispersion. While DLS is performed on nanoparticles in suspension, polydisperse nanoparticles or irregular and branched aggregates can lead to light scattering, which impairs the analysis by DLS. Nanoparticles have been analyzed by analytical ultracentrifugation, fluorescence correlation spectroscopy, and single-particle tracking,[11] but these methods are limited by rather slow operation and the requirement for demanding instrumentation. Filtration,[12] precipitation,[13,14] size-exclusion chromatography,[15,16] capillary electrophoresis,[17−19] and field-flow fractionation[15,16] were used for the size-dependent separation of nanomaterials. Filtration

Received: February 4, 2014
Accepted: April 3, 2014
Published: April 3, 2014

and precipitation, however, are better suited for the separation of higher quantities of nanoparticles with low resolution. High-resolution methods, such as chromatography, field-flow fractionation, and capillary electrophoresis, are not suitable for nanoparticles that strongly interact with the stationary phase or capillary wall because they may never reach the detector of the instrument.[20−22]

Gel electrophoresis is one of the most important tools for the analysis of biomolecules because it is fast and cost-effective and provides an excellent separation power.[23] Only recently, however, gel electrophoresis has been introduced for the analysis and fractionation of nanoparticles,[19,24,25] such as quantum dots,[26−28] nanoparticles modified by a discrete number of functional groups,[29,30] metallic nanoparticles, or DNA−gold nanoparticle assemblies.[31−33] The electrophoretic mobility of proteins and other biomolecules can be easily modified by the buffer composition,[23] which also facilitates the electrophoretic separation of nanoparticles and their bioconjugates.[11] Another advantage of gel electrophoresis compared to separation methods based on flow detectors (e.g., chromatography and field-flow fractionation) is the possibility to record a picture of the whole gel. The direct visualization of the separation path enables the analysis of many samples in parallel and simplifies the detection of nanoparticle aggregates. Finally, gel electrophoresis can provide simultaneous information on the nanoparticle diameter, charge, ζ potential, and free electrophoretic mobility.[34]

Despite this great potential, electrophoresis has only been used indirectly for analyzing the bioconjugation of UCNPs by separating excess reagents on a gel.[35,36] Here, we show that silica-coated UCNPs can be separated, detected, and purified directly on an agarose gel. To make this method widely available for the detection of any other type of silica or silica-coated nanoparticles, a new protocol has been developed for preparing fluorescein-doped silica without affecting the electrophoretic mobility. With this new analytical tool, UCNPs coated with either bare silica or carboxylated silica have been characterized in detail. The information obtained on the aggregation behavior has shown to be crucial in optimizing the design of a silica shell that yields a stable and monodisperse colloid and is amenable to subsequent bioconjugation steps.

2. EXPERIMENTAL PROCEDURES

2.1. Chemicals. Polyoxyethylene (5) nonylphenyl ether (Igepal CO-520), fluorescein 5(6)-isothiocyanate (FITC, >90%), (3-aminopropyl)triethoxysilane (APTES, 98%), *N*-(3-(dimethylamino)-propyl)-*N*′-ethylcarbodiimide hydrochloride (EDC, 98%), *N*-hydroxysulfosuccinimide sodium salt (Sulfo-NHS, ≥98%), bovine serum albumin (BSA, 98%), ammonium fluoride (ACS reagent, ≥98.0%), sodium hydroxide (reagent grade, ≥98.0%), *N*,*N*-dimethylformamide (DMF, ≥99.8%, dried over 3 Å molecular sieve), and bromophenol blue were purchased from Sigma-Aldrich (www.sigmaaldrich.com). Yttrium(III) chloride hexahydrate (99.99%), ytterbium(III) chloride hexahydrate (99.9%), erbium(III) chloride hexahydrate (99.9%), and gadolinium(III) chloride hexahydrate (99.99%) were from Treibacher (www.treibacher.at). Oleic acid (technical grade, 90%) and 1-octadecene (technical grade, 90%) were from Alfa Aesar (www.alfa.com). LE Agarose was from Lonza (www.lonza.com). Coomassie Brilliant Blue G-250 and 2-amino-2-hydroxymethylpropane-1,3-diol (Tris, p.a.) were from Serva (www.serva.de). Sodium dodecyl sulfate (SDS) was from Penta (www.pentachemicals.eu). Ammonia solution (25%) and tetraethyl orthosilicate (TEOS, 98%) were from Merck (www.merckmillipore.de). Cyclohexane (99.99%) was from Acros Organics (www.acros.com). Carboxyethylsilanetriol (CEST) sodium salt (25%) in water was from abcr (www.abcr.de).

2.2. Instruments. TEM images were taken on a 120 kV Philips CM12 microscope (www.fei.com); a copper carbon-coated 400-mesh grid with formvar membrane was used for nanoparticle deposition. Agarose gel electrophoresis was performed on a Mini-PROTEAN Tetra Companion Running Module (www.bio-rad.com). The agarose gels were documented on an InGenius gel imaging and analysis system (Syngene, www.syngene.com). The upconversion luminescence (UCL) of UCNP recovered from separate gel sections was measured on a custom-built CHAMELEON multilabel microplate reader from Hidex (www.hidex.com; 1.5 W laser excitation at 980 nm; 550 nm bandpass emission filter). DLS was performed on a Zetasizer (Malvern Instruments, www.malvern.com). The UCL spectra were recorded on a Cary Eclipse fluorescence spectrophotometer (Agilent Technologies, www.agilent.com) equipped with a 5 W, 980 nm laser. Fourier transform infrared (FTIR) spectra were recorded on a Varian 670-IR spectrometer equipped with a PIKE GladiATR.

2.3. Preparation of FITC−APTES Adduct. The FITC−APTES adduct was prepared following a previously described method.[37] APTES was amino-modified by fluorescein isothiocyanate (see Figure S1 of the Supporting Information): A solution of 19.2 μL of APTES (25 μL of APTES in 800 μL of DMF) was added to a solution of 0.5 mg of FITC in 400 μL of DMF. The mixture was incubated for 2 h at room temperature before further use.

2.4. Synthesis of Silica-Coated UCNPs by Reverse Microemulsion. Monodisperse UCNPs of 12 nm in diameter were prepared by high-temperature co-precipitation, as described earlier.[38] To generate the reverse microemulsion, typically 3.3 mg of UCNPs were first dispersed in a mixture of 500 μL of Igepal CO-520 in 10 mL of cyclohexane before 100 μL of 25% ammonium hydroxide was added. After stirring for 10 min, 15 μL of TEOS was added to the mixture, which was further stirred for 48 h in a sealed flask at room temperature for coating the UCNP with a bare silica shell (UCNP@Silica). Alternatively, 4.3 μL of FITC−APTES in DMF was added with 15 μL of TEOS to generate a fluorescently doped silica shell (UCNP@Silica−FITC). A constant molar ratio of TEOS/APTES/FITC (10 000:2:1) was used in all experiments.

UCNP coated with carboxylated silica (UCNP@Silica−COOH) or fluorescently doped carboxylated silica (UCNP@Silica−FITC−COOH) were prepared by adding 20 μL of CEST at 3 h after the addition of TEOS. After ultrasonication for 30 min, the reaction was further incubated for 45 h.

The nanoparticles were precipitated by adding 5 mL of acetone and collected by centrifugation (600*g*/10 min). They were washed 3 times using acetone (600*g*/10 min, sonication for 5 min). Bare silica nanoparticles were washed twice using a 2:1 (v/v) mixture of ethanol and water (13000*g*/15 min, sonication for 5 min) and dispersed in the ethanol/water mixture to yield a concentration of 15 mg mL^{-1}. Carboxylated particles were washed twice using water (13000*g*/15 min) and dispersed in water without sonication to yield a concentration of 15 mg mL^{-1}.

2.5. Agarose Gel Electrophoresis. Silica-coated UCNPs and their bioconjugates were separated on a vertical agarose gel [1.0−2.5% (w/v), 83 mm width and 70 mm height] using 45 mM Tris, 45 mM H_3BO_3, and 3 mM SDS at pH 8.6 as the electrophoresis buffer. (1) UCNPs dispersed in 27 μL of 67% (v/v) aqueous ethanol solution were mixed with 27 μL of glycerol and 6 μL of 30 mM SDS. (2) UCNPs dispersed in 12 μL of water were mixed with 12 μL of glycerol, 30 μL of water, and 6 μL of 30 mM SDS. The final UCNP concentration was approximately 3 mg mL^{-1}. The samples were sonicated for 10 min and loaded onto the gel pockets. Electrophoresis was typically carried out for 30 min under a constant voltage of 100 V. An image was taken of the slab gels under ultraviolet (UV) irradiation using a standard gel imaging system.

2.6. Recovery of UCNPs from Separate Gel Sections and Measurement of Their UCL. After electrophoresis, the agarose gels were cut into small strips of typically 2.5 mm width along the separation path. These strips were placed into wells of a microtiter plate, and 100 μL of buffer (45 mM Tris, 45 mM H_3BO_3, and 3 mM SDS at pH 8.6) was added and shaken overnight. A volume of 70 μL of buffer containing the resuspended UCNPs was pipetted into a new

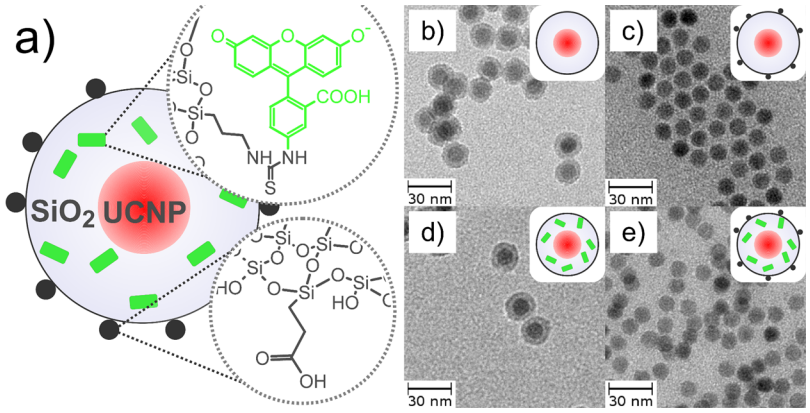

Figure 1. (a) Schematic drawing of silica-coated UCNPs. UCNPs were coated with either a (b) bare or (c) carboxylated (black dots) silica shell. In parallel approaches, fluorescein (green) was added to the (d) bare or (e) carboxylated silica shell.

microtiter plate to measure the UCL. The resuspended UCNPs were sonicated for 20 min before preparing the sample for taking TEM images.

3. RESULTS AND DISCUSSION

3.1. Design and Characterization of Silica-Coated UCNPs. Monodisperse UCNPs of 12 nm in diameter were coated with either a bare or carboxylated silica shell by reverse microemulsion, as shown in Figure 1.[39] In parallel approaches, each type of silica shell was doped with a fluorescein silane derivative (see Figure S1 of the Supporting Information) to render them visible by standard fluorescence instrumentation.

The UCNPs were characterized by recording UCL spectra, TEM, and DLS (see Figures S2–S12 of the Supporting Information). The bare silica shell has a thickness of 4 nm (panels b and d of Figure 1 and Figure S8 of the Supporting Information). Because the very thin carboxylated silica shell[39] is not visible in panels c and e of Figure 1, the presence of silica and/or carboxyl groups was confirmed by FTIR (see Figure S13 of the Supporting Information). TEM and DLS showed the same size and shape of UCNPs, independent of the fluorescent dopant. UCNPs coated with a bare silica shell, however, appear more aggregated in the TEM images and have a much larger hydrodynamic diameter (120 nm) compared to the carboxylated silica shell (30 nm). A similar aggregation of bare and surface-modified silica nanoparticles has also been observed by others.[7,8,39]

3.2. Separation and Purification of Silica-Coated UCNPs by Gel Electrophoresis. The four types of silica-coated UCNPs were subjected to agarose gel electrophoresis. Both silanol groups (pK_a = 7.0)[40] and carboxyl groups (pK_a = 4.5)[41] confer a homogeneous negative surface charge to the nanoparticles, which facilitates a size-dependent separation through gel electrophoresis. The concentration of agarose in the slab gel can be adjusted to the expected size of the nanoparticles, and 1.5–2.5% of agarose was found to be optimal for separating silica-coated UCNPs of 12 nm diameter. A standard electrophoresis buffer of low ionic strength and slightly alkaline pH was used to prevent nanoparticle aggregation.

The fluorescein-doped UCNPs are directly detectable in the gel slab under UV illumination (Figure 2). UCNPs coated with bare silica are located in several distinct bands, followed by a long diffuse zone and a fraction that has not entered the gel matrix. This electrophoretic pattern indicates several fractions

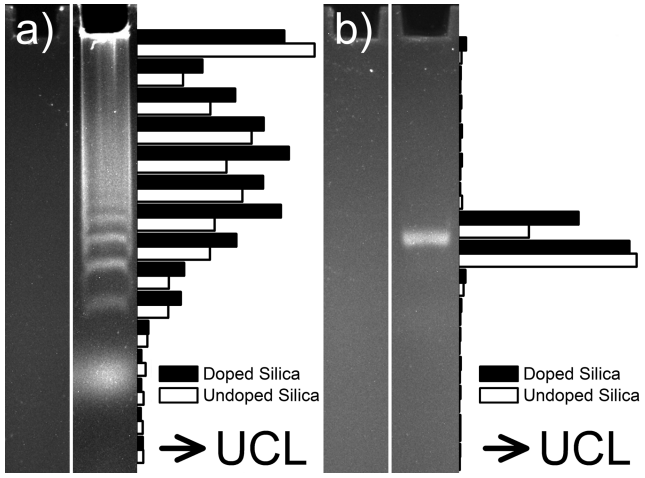

Figure 2. Agarose gel electrophoresis reveals nanoparticle aggregation. (a) UCNPs coated with a bare silica shell are separated in several distinct bands (1.5% agarose, 100 V, 30 min), which can be attributed to discrete clusters of UCNPs. (b) Carboxylated UCNPs form only a single well-defined band of monodisperse UCNPs (2.5% agarose, 100 V, 30 min). Each panel shows silica-coated UCNPs (left lane) without and (right lane) with fluorescein that are directly visible in the gel under UV illumination. The UCNPs were recovered in suspension from separate gel sections to determine the UCL. Essentially the same electrophoretic separation is observed for (full bars) fluorescently doped UCNPs and (empty bars) non-doped UCNPs.

of more or less aggregated nanoparticles. In contrast, UCNPs coated with a carboxylated silica shell are located in a well-defined band, thus indicating a single fraction of monodisperse nanoparticles. The slab gels were cut into thin slices to recover the nanoparticles from each slice in suspension and to determine their UCL. In this way, it was shown that (1) the fluorescent bands in the slab gel relate to the presence of UCNPs and (2) UCNPs without and with a fluorescent dopant migrate with the same electrophoretic mobility. Consequently, fluorescent doping affects neither the size, surface charge, nor aggregation of nanoparticles and can also be used for the electrophoretic characterization and detection of any other type of bare silica or silica-coated nanoparticles.

The recovered silica-coated UCNPs were inspected by TEM to confirm that individual bands in the gel relate to the presence of a discrete number of aggregated nanoparticles (Figure 3; for full TEM images, see Figures S14–S17 of the

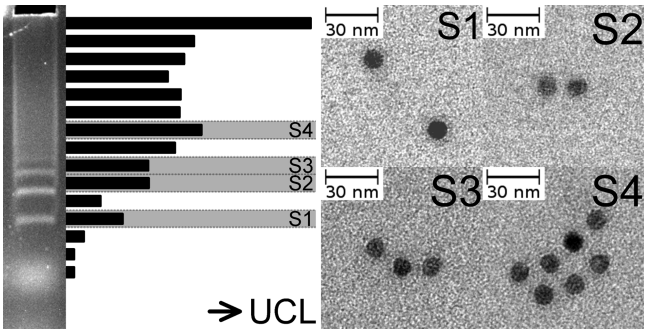

Figure 3. Correlation between electrophoretic mobility and aggregation of silica-coated UCNPs. After gel electrophoresis (1.5% agarose, 100 V, 30 min), silica-coated UCNPs can be identified in separate bands by the fluorescent dopant. The UCNPs are recovered in suspension from sections of the slab gel to record the UCL and take TEM images. Stable aggregates consisting of a discrete number of silica-coated nanoparticles that correlate to their electrophoretic mobility are found in gel sections S1−S4.

Supporting Information). Consequently, aggregates of silica-coated nanoparticles are not an artifact generated during the sample preparation for TEM but are already present in suspension. It should also be noted that this recovery from individual bands of the agarose gel provides a straightforward way to prepare highly purified and non-aggregated UCNPs or any other types of silica-coated nanoparticles. The fast identification of the bands in the gel is facilitated by the fluorescent dopant, which has no effect on the electrophoretic mobility.

3.3. Ferguson Analysis. The discrete number of aggregated nanoparticles in each band was further confirmed by a Ferguson analysis.[42] UCNPs coated with bare silica were separated on gels containing either 1.5 or 2.0% agarose. A linear relationship was observed between the square root of the retardation coefficient (K_r) and the number of UCNPs per aggregate in the well-defined bands of the agarose gels (Figure 4). In contrast, the more diffuse bands that migrate the longest distance (zones 1 and 2) display a similar electrophoretic mobility, irrespective of the agarose concentration, and have essentially the same K_r of 0.01 as the low-molecular-mass electrophoresis marker bromophenol blue (669.96 g mol^{-1}). We assume that zones 1 and 2 can be attributed to an excess of fluorescently labeled silica oligomers of low molecular weight that are not restricted by the agarose gel.

3.4. Gel Electrophoresis of UCNP Bioconjugates. UCNPs coated with a carboxylated silica shell that do not form aggregates in the first place and provide a functional group for bioconjugation were used for surface modification with the model protein BSA (see Figures S18−S20 of the Supporting Information). The nanoparticles were detectable in the gel by the fluorescent dopant, and BSA was directly visible by its autofluorescence (see Figure S21 of the Supporting Information). Figure 5 shows the UCNPs in the agarose gel (a) before and (b) after bioconjugation with an excess amount of BSA. The presence of UCNPs in a single well-defined band of each gel was confirmed by measuring the UCL in the gel sections. The electrophoretic mobility of the UCNPs, however, is strongly reduced after bioconjugation. The band that contains the monodisperse UCNPs after bioconjugation can be clearly distinguished from a second band of unreacted BSA. Consequently, the separated UCNP bioconjugates can be simply recovered from the slab gel to remove excess reagents that may interfere in subsequent bioanalytical applications.

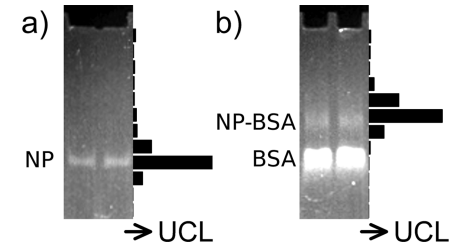

Figure 5. Bioconjugation of UCNPs. The binding of the model protein BSA onto the carboxylated silica shell of UCNPs can be detected by a shift in the electrophoretic mobility (1.5% agarose, 100 V, 25 min) (a) before and (b) after bioconjugation. (b) Fluorescently doped UCNPs and the autofluorescent BSA are visible as separate bands in the gel. The presence of UCNPs in the bands is confirmed by determining the UCL in the respective gel sections.

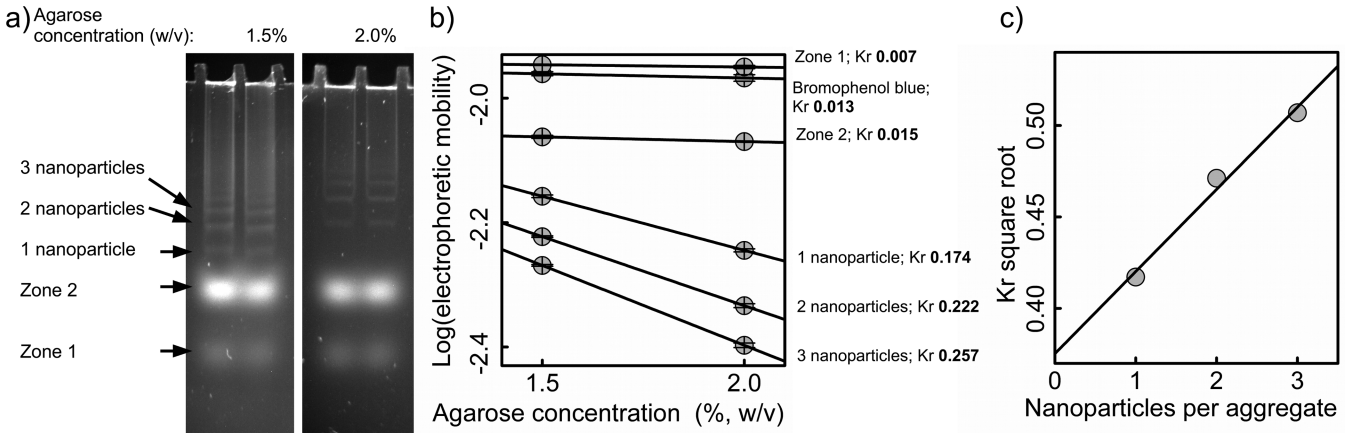

Figure 4. Ferguson analysis. (a) UCNPs coated with fluorescein-doped silica were separated in two differently concentrated agarose gels (1.5 and 2.0%, 100 V, 30 min). Only bands containing nanoparticles are retarded by the gel and show a shift in their electrophoretic mobility. (b) Calculation of the retardation coefficients K_r from a Ferguson plot. Bands containing nanoparticles or aggregates of nanoparticles display a K_r much higher than 0.01 and, thus, can be clearly distinguished from zones 1 and 2. (c) Square roots of K_r increase linearly, indicating that successive bands contain discrete numbers of one, two, and three nanoparticles.

4. CONCLUSION

Unlike the wealth of methods available for the analysis of small molecules, the toolbox for the characterization of nanoparticles is rather limited. Here, we have shown that, in addition to TEM and DLS, agarose gel electrophoresis is an important complementary tool for both analyzing and preparing highly purified silica-coated UCNPs. Electrophoresis is amenable to the identification and separation of aggregates consisting of a discrete number of silica-coated UCNPs. Furthermore, electrophoresis can be readily employed to monitor the growth of a silica shell on any other type of nanoparticles or to analyze silica nanoparticles doped with a fluorescent dye. Fluorescence staining and gel electrophoresis enable the detection of an extremely thin silica shell that is invisible by conventional TEM and controlling further surface (bio-)functionalization steps of the silica surface, which may impair the nanoparticle stability in suspension or lead to cross-linking and aggregation. With this fundamental study, we have also paved the way for a Ferguson analysis to estimate the size and surface charge of silica-coated nanoparticles (and their aggregates). Complementary methods, such as isoelectric focusing and two-dimensional (2D) electrophoresis, will provide further information on the isoelectric point, the formation of the "protein corona", and the interactions of nanoparticles with biomolecules. The analysis of nanoparticles will also benefit from recent progress in automation and miniaturization of gel electrophoresis.[43]

■ ASSOCIATED CONTENT

Ⓢ Supporting Information

Characterization of UCNPs by TEM, luminescence spectra, and FTIR, schemes of fluorescent adduct preparation and nanoparticle bioconjugation, and protein detection on agarose gels by fluorescence. This material is available free of charge via the Internet at http://pubs.acs.org.

■ AUTHOR INFORMATION

Corresponding Author

*Telephone: +49-941-943-4015. Fax: +49-941-943-4064. E-mail: hans-heiner.gorris@ur.de.

Notes

The authors declare no competing financial interest.

■ ACKNOWLEDGMENTS

The authors acknowledge funding by the Program of "Employment of Newly Graduated Doctors of Science for Scientific Excellence" (Grant CZ.1.07/2.3.00/30.0009), co-financed by the European Social Fund and the state budget of the Czech Republic, and the German Academic Exchange Service (DAAD).

■ REFERENCES

(1) Haase, M.; Schäfer, H. Upconverting nanoparticles. *Angew. Chem. Int. Ed.* **2011**, *50*, 5808−5829.

(2) Gorris, H. H.; Wolfbeis, O. S. Photon-upconverting nanoparticles for optical encoding and multiplexing of cells, biomolecules, and microspheres. *Angew. Chem., Int. Ed.* **2013**, *52*, 3584−3600.

(3) Gorris, H. H.; Ali, R.; Saleh, S. M.; Wolfbeis, O. S. Tuning the dual emission of photon-upconverting nanoparticles for ratiometric multiplexed encoding. *Adv. Mater.* **2011**, *23*, 1652−1655.

(4) Guerrero-Martínez, A.; Pérez-Juste, J.; Liz-Marzán, L. M. Recent progress on silica coating of nanoparticles and related nanomaterials. *Adv. Mater.* **2010**, *22*, 1182−1195.

(5) Selvin, P. R.; Rana, T. M.; Hearst, J. E. Luminescence resonance energy transfer. *J. Am. Chem. Soc.* **1994**, *116*, 6029−6030.

(6) Ding, H. L.; Zhang, Y. X.; Wang, S.; Xu, J. M.; Xu, S. C.; Li, G. H. Fe_3O_4@SiO_2 core/shell nanoparticles: The silica coating regulations with a single core for different core sizes and shell thicknesses. *Chem. Mater.* **2012**, *24*, 4572−4580.

(7) Bagwe, R. P.; Hilliard, L. R.; Tan, W. Surface modification of silica nanoparticles to reduce aggregation and nonspecific binding. *Langmuir* **2006**, *22*, 4357−4362.

(8) Nooney, R. I.; McCormack, E.; McDonagh, C. Optimization of size, morphology and colloidal stability of fluorescein dye-doped silica NPs for application in immunoassays. *Anal. Bioanal. Chem.* **2012**, *404*, 2807−2818.

(9) Liebherr, R. B.; Soukka, T.; Wolfbeis, O. S.; Gorris, H. H. Maleimide activation of photon upconverting nanoparticles for bioconjugation. *Nanotechnology* **2012**, *23* (48), 485103.

(10) Wilhelm, S.; Hirsch, T.; Patterson, W. M.; Scheucher, E.; Mayr, T.; Wolfbeis, O. S. Multicolor upconversion nanoparticles for protein conjugation. *Theranostics* **2013**, *3*, 239−248.

(11) Sapsford, K. E.; Tyner, K. M.; Dair, B. J.; Deschamps, J. R.; Medintz, I. L. Analyzing nanomaterial bioconjugates: A review of current and emerging purification and characterization techniques. *Anal. Chem.* **2011**, *83*, 4453−4488.

(12) Krieg, E.; Weissman, H.; Shirman, E.; Shimoni, E.; Rybtchinski, B. A recyclable supramolecular membrane for size-selective separation of nanoparticles. *Nat. Nanotechnol.* **2011**, *6*, 141−146.

(13) Borchert, H.; Talapin, D. V.; Gaponik, N.; McGinley, C.; Adam, S.; Lobo, A.; Möller, T.; Weller, H. Relations between the photoluminescence efficiency of CdTe nanocrystals and their surface properties revealed by synchrotron XPS. *J. Phys. Chem. B* **2003**, *107*, 9662−9668.

(14) Mastronardi, M. L.; Maier-Flaig, F.; Faulkner, D.; Henderson, E. J.; Kübel, C.; Lemmer, U.; Ozin, G. A. Size-dependent absolute quantum yields for size-separated colloidally-stable silicon nanocrystals. *Nano Lett.* **2012**, *12*, 337−342.

(15) Fedotov, P. S.; Vanifatova, N. G.; Shkinev, V. M.; Spivakov, B. Y. Fractionation and characterization of nano- and microparticles in liquid media. *Anal. Bioanal. Chem.* **2011**, *400*, 1787−1804.

(16) Kowalczyk, B.; Lagzi, I.; Grzybowski, B. A. Nanoseparations: Strategies for size and/or shape-selective purification of nanoparticles. *Curr. Opin. Colloid Interface Sci.* **2011**, *16*, 135−148.

(17) Carrillo-Carrión, C.; Moliner-Martínez, Y.; Simonet, B. M.; Valcárcel, M. Capillary electrophoresis method for the characterization and separation of CdSe quantum dots. *Anal. Chem.* **2011**, *83*, 2807−2813.

(18) Liu, F.-K.; Lin, Y.-Y.; Wu, C.-H. Highly efficient approach for characterizing nanometer-sized gold particles by capillary electrophoresis. *Anal. Chim. Acta* **2005**, *528*, 249−254.

(19) Pyell, U. Characterization of nanoparticles by capillary electromigration separation techniques. *Electrophoresis* **2010**, *31*, 814−831.

(20) Bi, Y.; Pan, X.; Chen, L.; Wan, Q.-H. Field-flow fractionation of magnetic particles in a cyclic magnetic field. *J. Chromatogr., A* **2011**, *1218*, 3908−3914.

(21) Yu, C. J.; Su, C. L.; Tseng, W. L. Separation of acidic and basic proteins by nanoparticle-filled capillary electrophoresis. *Anal. Chem.* **2006**, *78*, 8004−8010.

(22) Wei, G. T. Shape separation of nanometer gold particles by size-exclusion chromatography. *Anal. Chem.* **1999**, *71*, 2085−2091.

(23) Westermeier, R. *Electrophoresis in Practice*, 4th ed.; Wiley-VCH: Weinheim, Germany, 2005.

(24) Surugau, N.; Urban, P. L. Electrophoretic methods for separation of nanoparticles. *J. Sep. Sci.* **2009**, *32*, 1889−1906.

(25) López-Lorente, A. I.; Simonet, B. M.; Valcárcel, M. Electrophoretic methods for the analysis of nanoparticles. *TrAC, Trends Anal. Chem.* **2011**, *30*, 58−71.

(26) Parak, W. J.; Gerion, D.; Zanchet, D.; Woerz, A. S.; Pellegrino, T.; Micheel, C.; Williams, S. C.; Seitz, M.; Bruehl, R. E.; Bryant, Z.; Bustamante, C.; Bertozzi, C. R.; Alivisatos, A. P. Conjugation of DNA

to silanized colloidal semiconductor nanocrystalline quantum dots. *Chem. Mater.* **2002**, *14*, 2113−2119.
(27) Hlavacek, A.; Bouchal, P.; Skládal, P. Biotinylation of quantum dots for application in fluoroimmunoassays with biotin−avidin amplification. *Microchim. Acta* **2012**, *176*, 287−293.
(28) Hlavacek, A.; Skládal, P. Isotachophoretic purification of nanoparticles: Tuning optical properties of quantum dots. *Electrophoresis* **2012**, *33*, 1427−1430.
(29) Sperling, R. A.; Pellegrino, T.; Li, J. K.; Chang, W. H.; Parak, W. J. Electrophoretic separation of nanoparticles with a discrete number of functional groups. *Adv. Funct. Mater.* **2006**, *16*, 943−948.
(30) Zhang, T.; Yang, Z.; Liu, D. DNA discrete modified gold nanoparticles. *Nanoscale* **2011**, *3*, 4015−4021.
(31) Mastroianni, A. J.; Claridge, S. A.; Alivisatos, A. P. Pyramidal and chiral groupings of gold nanocrystals assembled using DNA scaffolds. *J. Am. Chem. Soc.* **2009**, *131*, 8455−8459.
(32) Parak, W. J.; Pellegrino, T.; Micheel, C. M.; Gerion, D.; Williams, S. C.; Alivisatos, A. P. Conformation of oligonucleotides attached to gold nanocrystals probed by gel electrophoresis. *Nano Lett.* **2003**, *3*, 33−36.
(33) Hanauer, M.; Pierrat, S.; Zins, I.; Lotz, A.; Sönnichsen, C. Separation of nanoparticles by gel electrophoresis according to size and shape. *Nano Lett.* **2007**, *7*, 2881−2885.
(34) Park, S.; Hamad-Schifferli, K. Evaluation of hydrodynamic size and zeta-potential of surface-modified Au nanoparticle−DNA conjugates via Ferguson analysis. *J. Phys. Chem. C* **2008**, *112*, 7611−7616.
(35) Jiang, S.; Zhang, Y.; Lim, K. M.; Sim, E. K. W.; Ye, L. NIR-to-visible upconversion nanoparticles for fluorescent labeling and targeted delivery of siRNA. *Nanotechnology* **2009**, *20* (15), 155101.
(36) Yang, Y.; Liu, F.; Liu, X.; Xing, B. NIR light controlled photorelease of siRNA and its targeted intracellular delivery based on upconversion nanoparticles. *Nanoscale* **2013**, *5*, 231−238.
(37) van Blaaderen, A.; Vrij, A. Synthesis and characterization of colloidal dispersions of fluorescent, monodisperse silica spheres. *Langmuir* **1992**, *8*, 2921−2931.
(38) Wang, F.; Han, Y.; Lim, C. S.; Lu, Y.; Wang, J.; Xu, J.; Chen, H.; Zhang, C.; Hong, M.; Liu, X. Simultaneous phase and size control of upconversion nanocrystals through lanthanide doping. *Nature* **2010**, *463*, 1061−1065.
(39) Liu, F.; Zhao, Q.; You, H.; Wang, Z. Synthesis of stable carboxy-terminated $NaYF_4$:Yb^{3+},Er^{3+}@SiO_2 nanoparticles with ultrathin shell for biolabeling applications. *Nanoscale* **2013**, *5*, 1047−1053.
(40) Kosmulski, M. The pH-dependent surface charging and the points of zero charge. *J. Colloid Interface Sci.* **2002**, *253*, 77−87.
(41) Labéguerie-Egéa, J.; McEvoy, H. M.; McDonagh, C. Synthesis, characterisation and functionalisation of luminescent silica nanoparticles. *J. Nanopart. Res.* **2011**, *13*, 6455−6465.
(42) Ferguson, K. A. Starch-gel electrophoresis—Application to the classification of pituitary proteins and polypeptides. *Metab. Clin. Exp.* **1964**, *13*, 985−1002.
(43) Hughes, A. J.; Herr, A. E. Microfluidic Western blotting. *Proc. Natl. Acad. Sci. U. S. A.* **2012**, *109*, 21450−21455.